1996

Mechanical Alloying of Nitrogen into Iron Powders

J. Rawers

D. Govier

D. Cook
Old Dominion University, dccook@odu.edu

Original Publication Citation

Rawers, J., Govier, D., & Cook, D. (1996). Mechanical alloying of nitrogen into iron powders. *ISIJ International, 36*(7), 958-961. doi:10.2355/isijinternational.36.958

ISIJ International, Vol. 36 (1996), No. 7, pp. 958–961

Mechanical Alloying of Nitrogen into Iron Powders

J. RAWERS, D. GOVIER and D. COOK[1)]

U. S. Bureau of Mines, Albany, Oregon, USA. 1) Old Dominion University, Norfolk, Virginia, USA.

(Received on October 6, 1995; accepted in final form on March 4, 1996)

Mechanical alloying of nitrogen into bcc-Fe powder is a very effective and efficient means of obtaining very high concentration of nitrogen in micron-size iron particles. Mechanical alloying increases the concentration of nitrogen in the iron powder far in excess of the bcc-Fe lattice low nitrogen solubility, however most of the infused nitrogen resides on the nano-size grain boundaries and in nano-size bct-Fe that forms during mechanical alloying.

KEY WORDS: mechanical alloying; iron; nitrogen.

1. Introduction

Addition of nitrogen to bcc-Fe alloys is very difficult. Because nitrogen is a gas and its solubility in bcc-Fe iron is very limited, many of the techniques used to alloy metallic elements into iron are not applicable. Currently there are a limited number of techniques that can be used to enhance the nitrogen concentration in bcc-iron alloys. In a previous presentation at this conference, the benefits of HIGH-PRESSURE MELTING—in excess of 200 MPa—were discussed and shown to increase the nitrogen concentration in iron in excess of 1.5 wt%. However this high level of nitrogen was accompanied by the formation of Fe_4N. For the pressures currently used in commercially produced steel castings (<5 MPa), the nitrogen solubility in bcc-Fe is less than 0.15 (wt%).[2)] Other nitridation techniques such as ion-implant and solid state diffusion are limited to near surface alloying, and are not applicable to bulk nitridation.

As an alternative to adding nitrogen to molten iron or to the near surface of large pieces, nitrogen can be readily added (i) to the molten metal prior to or during the atomization process,[3)] and to iron powders: (ii) by solid state diffusion,[2,4)] or (iii) during mechanical alloying by processing in a nitrogen environment[5)] or by alloying with metal nitrides.[6)] These nitrogen enhanced powders can then be consolidated by a number of techniques such as: explosive compaction,[3)] HIP,[7)] hot-extrusion,[3)] *etc.* In a later presentation at this conference, the advantages—such as: full-density and retention of nanostructure—and limitations of each of these techniques—such as: sample size and cost—are discussed. This presentation will describe nitrogen addition to iron powder by mechanical processing iron powder in a nitrogen environment.

Several studies have used mechanical alloying, to produce nitrogen-enhanced powders[6,7)] including one described at the HNS-90 conference.[9)] This study describes the addition of nitrogen to bcc-Fe powder during attrition ball-milling by the processing of iron powder in a nitrogen gas atmosphere. The resulting powder is a highly strained, micron-size particles with nanocrystalline grains. The resulting micro- and nanostructure and nitrogen distribution will be characterized using X-ray diffraction and Mössbauer data.

During attrition ball-milling, iron powder is subjected to high impact energy between colliding steel balls. The powder particles are deformed, cold-worked, and eventually fragments.[10–12)] With subsequent processing the fragmented particles are cold-welded (**Fig. 1**). The amount of fragmentation and the number of cold-weldments increases with increasing processing time. When the iron particles deform and/or fragment, fresh metal is exposed to the surrounding nitrogen gas environment. Nitrogen gas molecules are readily adsorbed onto the iron surface where they rapidly dissociates and develops a firm, chemical bond between the nitrogen

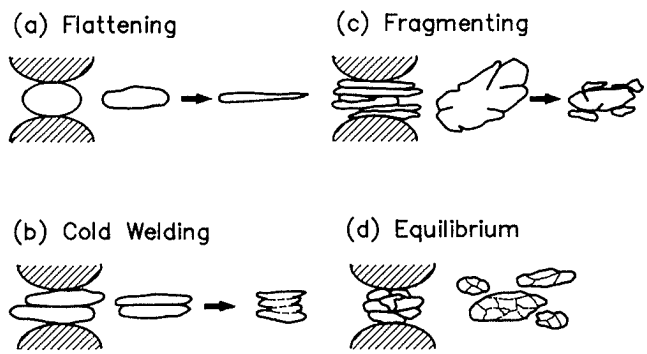

Fig. 1. Schematic of mechanical alloying process.
(a) initial processing: extensive cold-working during particle flattening
(b) with continued processing: particles become cold-welded together
(c) with continued processing: particles begin to fragment
(d) with continued processing: continued fragmentation and cold-welding produces micronsize particles with equiaxed nanograins.

atoms and the iron surface.[13,14] When these gas coated surfaces are cold-welded together the surface now becomes trapped inside the particle and becomes part of the newly formed, internal, grain structure of the powder particle. This process eventually results in an equiaxed, micron-size particle with nanocrystalline grains.

In this study iron powder was processed in both an argon and a nitrogen gas environment. The resulting milled particles were analyzed by electron microscopy, X-ray diffraction (XRD), and Mössbauer to determine (i) the effect(s) of mechanical processing iron powder in an inert environment, (ii) the additional effect(s) that results from processing in a nitrogen gas environment, and (iii) the effect of mechanically infused nitrogen alloy might have on the final grain structure. Mössbauer analysis characterizes the interatomic structure, XRD analysis characterizes the nano-structure, and electron microscopy characterized the micro-structure.

2. Experimentation

Mechanical processing of approximately 500 g of elemental iron powder (30–50 micrometer in diameter and 99.7% pure) was done in a ATTRITOR ball mill using 5 mm, 440°C stainless steel balls. Rotational speed was approximately 300PRM. The ball-to-powder ratio was approximately 20 : 1. Processing time was 150 h. Processing chamber was maintained under a positive pressure of approximately 100 m*l* above atmospheric with either argon or nitrogen gas. Samples (10—25 g) were removed after 8, 25, 50, 75, 100, and 150 h. Mechanically processed powders were then analyzed for chemical composition (LECO TC436 Oxygen and Nitrogen analyzer) and microstructure (both X-ray diffraction, Mössbauer analysis). Details of the powder characteristic are presented in **Tables 1** and **2**. Further details including SEM and TEM analysis of the processed powder can be found in Refs. 1), 2), 7), and 8).

3. Discussion

After 150 h of processing the particle size decreased from 30–50 micrometer in diameter to 5–7 micrometers (**Fig. 2**). Electron micrography shows that the grain size was approximately uniform and that the individual grains contained few dislocations or twins. High resolution microscopy showed that the grains boundaries were high-angle and firm bonding between the grains.

Processing iron powder in a nitrogen gas environment resulted in a linear increase in nitrogen concentration with increasing processing times (**Fig. 3**). After 150 h of processing, nitrogen concentrations in excess of 1 wt% were obtained. Even though this concentration is far in excess of the nitrogen solubility limit, neither diffraction nor Mössbauer analysis showed the presence of any nitrides. Line shape analysis was conducted on the XRD Fe-(110) peak for grain size and internal strain (**Fig. 4**). During the first 25 h of processing the peak shape broadened. Deconvolution showed the presence of two peaks at approximately the same lattice d-spacing: one very broad, the other very narrow (similar to the as-received line shape). Single line Fourier analysis was used to determine grain size and strain of each deconvoluted lines. With increasing processing the intensity of the narrow line decreased and the broad peak

Table 1. Total nitrogen concentration, particle size, and X-ray diffraction analysis (phase composition, lattice d-spacing of Fe(110) plane, line full width at half maximum (FWHM), grain size, strain, and relative intensity of the phase) of mechanically processed iron powder processed in a nitrogen gas environment as a function of processing time.

time, hrs	8	25	50	75	100	150
nitrogen, wt%	0.017	0.148	0.385	0.610	0.82	1.19
particle size, mm	30.5	43.6	13.0	8.7	6.5	6.7
phases present	α, α*	α, α*	α*	α*, α'	α*, α'	α*, α'
as -received bcc-Fe (110) lattice plane: (α)						
d-spacing, nm	0.2026	0.2029	-.--			
FWHM (2Θ)	0.30	0.74				
grain size, nm	276	106				
strain, (%)	0.12	0.42				
cold - worked bcc-Fe (110) lattice plane: (α*)						
d-spacing, nm	0.2027	0.2030	0.2030	0.2030	0.2031	0.2033
FWHM (2Θ)	0.86	0.98	1.02	1.09	1.11	1.32
grain size, nm	9.4	8.8	6.9	7.1	6.9	5.8
strain, (%)	0.51	0.50	0.50	0.63	0.63	0.77
bct-Fe (101) lattice plane: (α')						
d-spacing, nm	-.--	-.--	-.--	0.2058	0.2069	0.2084
FWHM (2Θ)				3.96	3.52	3.46
grain size, nm				1.4	1.7	1.7
strain, (%)				0.0	0.0	0.0
rel intens, (%)				11	13	18

Table 2. Composite of the Mössbauer analysis from three different laboratories: C = Dr. Desmond Cook, Old Dominion University, Norfolk, Virginia, USA., G–F = Drs. Genin and Fall, Group de Spectrometrie Mössbauer, Nancy, France, and N = Dr. V. Nadutov, Institute for Metal Physics, Keiv, Ukraine. Interpretation of their results are that of the author.

atomic neighbor configuration	Material	Laboratory	H kOe	Isomer shift mm/s	Quadruple splitting mm/s	Width mm/s	rel. intens %
no nearest neighbors defect	Fe (foil)	N	330	0.001	-0.002	0.258	100
	Fe (powder)	N	332	-0.003	-0.003	0.276	100
	Fe-[Ar] 100	N	332	0.004	-0.004	0.34	84
		G-F	333	0.005	0.000	0.36	87
0-nn	Fe-[N] 100	N	333	0.006	0.002	0.35	71
		G-F	333	0.02	0.00	0.40	84
		C	332	0.01	0.0	---	83
first nearest neighbor defect 1 - nn	Fe-[Ar] 100	N	304	0.013	-0.037	0.35	10
		G-F	307	0.005	-0.011	0.48	16
	Fe-[N] 100	N	304	0.080	0.013	0.64	13
		G-F	310	0.03	0.007	0.33	9
		C	299	0.13	-0.01	---	7
next nearest neighbor 1*-nnn	Fe-[N] 100	N	354	0.15	-0.016	0.34	4
		G-F	345	0.02	0.0	0.31	16
		C	353	0.05	0.0	---	2
more than one nearest neighbor 2 - nn	Fe-[Ar] 100	N	279	-0.027	-0.22	0.45	4
	Fe-[N] 100	N	270	0.14	0.021	0.64	9
			255	0.14	0.27	0.81	6
		G-F	285	0.11	-0.07	0.89	27
		C	264	0.02	-0.10	---	3
			263	0.06	0.29	---	3

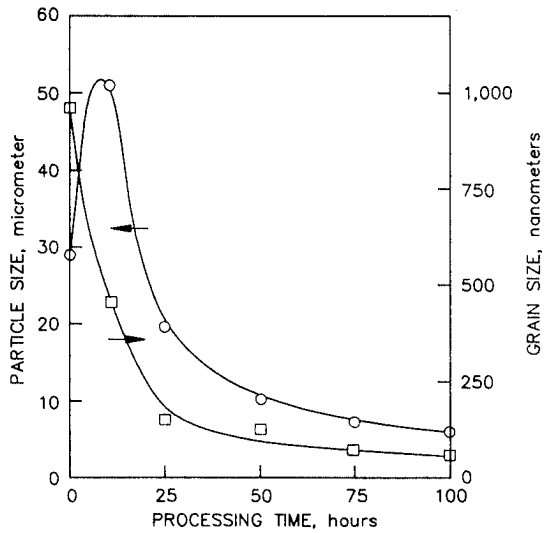

Fig. 2. Particle size (μm) and grain size (nm) as a function of processing time. Initial increase in particle size reflects the increase in particle size due to particle flattening.

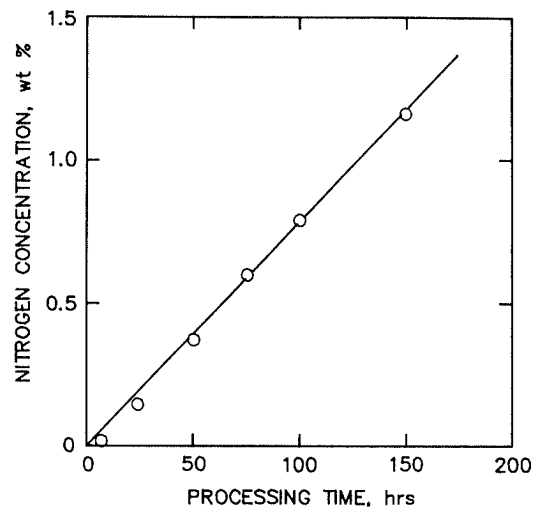

Fig. 3. Nitrogen concentration in mechanically processed powder as a function of processing time.

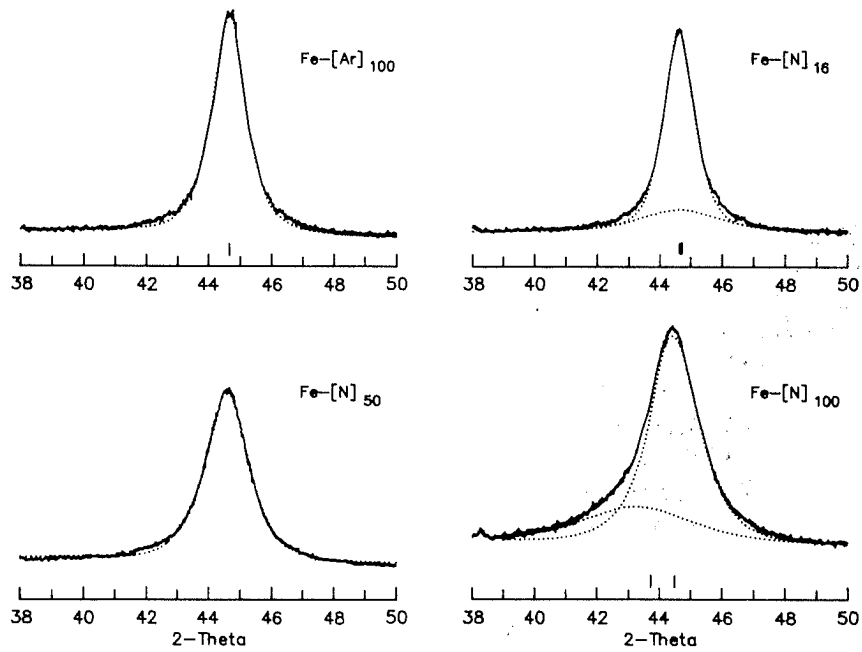

Fig. 4. Line deconvolution of Fe-(110) mechanically alloy peak and development of the bct-Fe (101) peak as a function of mechanical processing time. At 16 h of processing (Fe–$[N]_{16}$) the powder consist of two grain structures: as-received and cold-worked particles. At 50 h of processing (Fe–$[N]_{50}$) all the particles are cold-worked. At 100 h of processing (Fe–$[N]_{100}$) a second phase bct-Fe has started to develop.
Note: The equilibrium microstructure of the attrition mill machine is reflected in the powders processed for 100 h in argon (Fe–$[Ar]_{100}$).

increased. Analysis showed this peak to be associated with a heavily cold worked microstructure (Table 1). At around 50 h of processing only the wide peak remained. The cold-worked grain size was approximately 10 nm and the internal strain was approximately 0.8%. For iron powder processed in argon, little microstructure change occurred during the remainder of the processing.

However, for the powder processed in a nitrogen gas environment, after the cold-work structure had reached the limit of the attrition mill (as defined by the powder processed in argon), X-ray analysis showed a second peak began to form (Fig. 4). This peak was not at the same lattice d-spacing as the bcc-Fe peak but was adjacent to the bcc-Fe peak and continued to separate and grow in intensity with increasing processing time (Table 1). Examination of extended XRD patterns (20°–150°, Θ–2Θ) showed that each of the bcc-Fe peaks had developed a bct-Fe peak.

This new peak was initially interpret as either a second bcc-Fe phase developing or the development of a bct-Fe phase with the a-axis of the bcc- and bct-Fe being approximately the same, and the c-axis of the bct-Fe increasing. Mössbauer analysis was used to further understand the developing nanostructure (**Fig. 5**). Mössbauer analysis for the powder processed in argon for 150 h showed the presence of the bcc-Fe sextet and

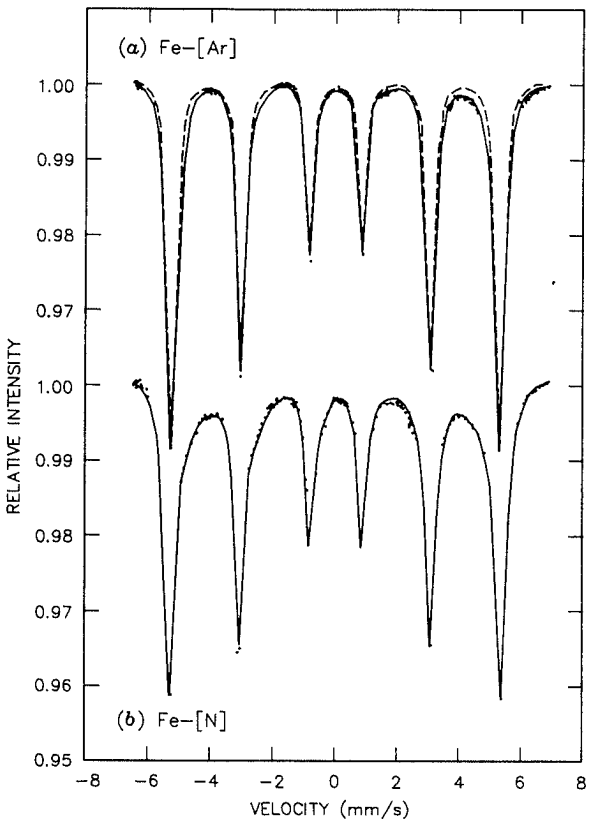

Fig. 5. Mössbauer spectra of iron powder processed in argon (Fe–[Ar]) and nitrogen (Fe–[N]) for 150 h. The Mössbauer pattern for unprocessed iron powder is shown as a dashed line in the Fe–[Ar] Mössbauer pattern.

a second sextet associated with small amount of disturbed microstructure (missing the first nearest neighbor). Mössbauer analysis for the powder processed in nitrogen for 150 h showed the presence of bcc-Fe with a small amount of disturbed microstructure, and the presence of sextets previously identified[9,15,16] as belonging to nitrogen enhanced bct-Fe (Table 2).

Analysis of the lattice d-spacing showed very little difference in the (110)-Fe lattice d-spacing of the powders processed in argon and powders in nitrogen and thus did not support the idea that much of the mechanically infused nitrogen had diffusion into the nano-size, bcc-Fe grains, and neither the X-ray diffraction nor the Mössbauer analysis showed the presence of any nitride second phase. Thus, the majority of nitrogen that was incorporated into the particles during mechanical alloying remained associated with the grain boundary after the particles were welded together. After the particles had reached their cold-work size limit (after approximately 50 h of processing), the further increase in nitrogen resulted in the formation of bct-Fe. The more open microstructure of the bct-Fe could now absorb the increase in nitrogen and reduce the strain imposed upon the lattice and grain boundary by the mechanical alloying and the presence of nitrogen.

4. Summary

Mechanical alloying of elemental bcc-Fe powder in a nitrogen atmosphere results in micrometer size particles with nano-size grains. Nitrogen infusion into the particles occurs by the nitrogen gas adsorption and dissociation onto the surface of particles and subsequent cold-welding of the particles together. The nitrogen remains on the grain boundary and when the nitrogen level and the cold-work microstructure reaches saturation, further addition of nitrogen results in the formation of nanocrystalline bct-Fe.

REFERENCES

1) J. Rawers: HNS '95.
2) J. Rawers, K. Frisk and D. Govier: *Mater. Sci. Eng. A*, **177A** (1994), 243.
3) J. Duning, J. Simmons and V. Sikka: Properties of High Nitrogen Steel Produced by High Pressure Atomization, HNS '95.
4) H. Feichtinger, A. Satir-Kolorz and Z. Xiao-hong: HNS '88 Conf., Lille, France, 75.
5) C. Doğan, J. Rawers, D. Govier and G. Korth: *Nanost. Mater.*, **4** (1994), 631.
6) J. Foct and R. de Figueiredo: *Nanost. Mater.*, **4** (1994), 685.
7) J. Rawers and R. Doan: *Metall. Mater. Trans. A*, **25** (1994), 381.
8) J. Rawers, D. Govier and D. Cook: *Scr. Metall. Mater.*, **32** (1995), 1319.
9) J. Foct, P. Rochegude and A. Mastorakis: HNS '90 Conf., Aachen, Germany, 72.
10) B. Aikin and T. Courtney: *Metall. Trans. A*, **24A** (1993), 647.
11) D. Maurice and T. Courtney: *Metall. Trans. A*, **21A** (1990), 289.
12) J. Rawers and D. Maurice: Accepted for publication *Scr. Metall. Mater.*, (1995).
13) C. Rettner, H. Pfnur, H. Stein and D. Augrbach: *J. Vac. Sci. Tech.*, **6A** (1988), 899.
14) J. Botteim W. Breng, T. Engel and U. Leuthausser: *Surf. Sci.*, **131** (1983), 258.
15) J. Genin and I. Fall: HNS '93 Conf., Kiev, Ukraine, 261.
16) V. Gavriljuk, V. Nadutov, M. Byelous and V. Kononngnko: NHS '90 Conf., Aachen, Germany, (1990).